

Dual Exponential Coupled Cluster Theory: Unitary Adaptation, Implementation in the Variational Quantum Eigensolver Framework and Pilot Applications

Dipanjali Halder¹, V. S. Prasanna², Rahul Maitra^{1,†}

¹ *Department of Chemistry,*

Indian Institute of Technology Bombay, Powai, Mumbai 400076, India

² *Centre for Quantum Engineering, Research and Education, TCG CREST, Salt Lake, Kolkata 700091, India*

[†] *rmaitra@chem.iitb.ac.in*

(Dated: 13 July 2022)

In this paper, we have developed a unitary variant of a double exponential coupled cluster theory, which is capable of mimicking the effects of connected excitations of arbitrarily high rank, using only rank-one and rank-two parametrization of the wavefunction ansatz. While its implementation in a classical computer necessitates the construction of an effective Hamiltonian which involves infinite number of terms with arbitrarily high many-body rank, the same can easily be implemented in the hybrid quantum-classical variational quantum eigensolver framework with a reasonably shallow quantum circuit. The method relies upon the nontrivial action of a unitary, containing a set of rank-two scattering operators, on entangled states generated via cluster operators. We have further introduced a number of variants of the ansatz with different degrees of expressibility by judiciously approximating the scattering operators. With a number of applications on strongly correlated molecules, we have shown that all our schemes can perform uniformly well throughout the molecular potential energy surface without significant additional implementation cost and quantum complexity over the unitary coupled cluster approach with single and double excitations.

I. INTRODUCTION

The emerging field of quantum computation has gained substantial attention due to its promise to solve certain computational problems that are difficult to handle with classical computers^{1–4}. Simulation of many body quantum systems is considered to be one such strenuous task owing to the exponential overhead of computational resources, thus limiting its application to small chemical systems. Unlike exact classical methods like full configuration interaction (FCI) that scales exponentially with system size, quantum algorithms such as quantum phase estimation (QPE) can tackle such problems with polynomial overhead. An overview of the developments in this field can be found in relevant review articles^{5,6}.

Earlier quantum computational algorithms to simulate molecular energies were based on the QPE approach as envisioned by Abrams and Lloyd^{7,8}. The objective of the phase estimation approach is to extract eigenvalues of a unitary operator by projecting the input state onto an eigenstate, provided the input state has substantial overlap with the exact eigenstate of the unitary operator. In 2005, Aspuru Guzik *et al.*⁹ first employed the phase estimation algorithm to simulate ground state energies of a few molecular systems. Eventually, Hefeng Wang and co-workers estimated excited state energies employing multiconfigurational self-consistent field (MC-SCF) wavefunction in the framework of QPE¹⁰. Apart from these papers, there have been numerous works in the QPE literature which deal with techniques for preparation of initial states suitable for the phase estimation approach, for example, see Ref.^{11–13}. Although it offers an

exponential speedup over the exact classical algorithms, QPE fails to meet the expectations of the near term noisy intermediate scale quantum (NISQ) devices owing to the requirement of long coherence times.

To circumvent this problem, a hybrid classical-quantum approach, namely variational quantum eigensolver (VQE) was proposed by Peruzzo and co-workers¹⁴. The idea stems from the Rayleigh-Ritz variational principle¹⁵, which dates back to early 1900s. VQE utilizes a combination of both classical and quantum architectures to find the best variational approximation to the ground state of a given Hamiltonian corresponding to a chosen trial wavefunction ansatz. Till date, VQE has been experimentally implemented in various quantum hardware architectures, viz. photonic quantum processors¹⁴, superconducting quantum processors^{16,17}, trapped ion architectures^{18–20} etc. It is worth mentioning at this point that the selection of a suitable wavefunction ansatz plays a pivotal role in the performance of VQE. In recent times, there have been a number of developments to formulate an expressive and cost efficient ansatz for VQE. An extensively used ansatz is the chemically motivated unitary coupled cluster ansatz, abbreviated as UCC^{14,21–25}. A generalized extension of the unitary coupled cluster ansatz truncated at singles and doubles excitations (UCCGSD), inspired from the earlier works of Nakatsuji²⁶ and Nooijen²⁷, has been studied by Van Voorhis and Head-Gordon²⁸, and further implemented in the VQE framework by Lee *et al.*²⁹. UCCGSD is considered to be the most expressive ansatz to date, but the expressibility comes at the expense of much higher scaling in terms of the number of parameters and the circuit depth (in comparison to UCCSD).

In the same paper, Lee and co-workers have further proposed an ansatz, termed as UpCCGSD, which is analogous to the UCCGSD ansatz, except for an added constraint of inclusion of *only generalized paired excitations* in the definition of two-body operators. UpCCGSD has been found to scale linearly against the system size, thus leading to a synergy between efficiency (in terms of cost of implementation), expressibility and the accuracy. The authors further showed that one may reach chemical accuracy across the potential energy surface of strongly correlated molecules with UpCCGSD ansatz by repeating the UpCCGSD circuit k number of times. This leads to k -fold increase of the circuit depth which anyway scales linearly against the system size. The same train of thought has led to the development of multireference unitary coupled cluster with partially generalized singles and doubles (MR-UCCpGSD) ansatz³⁰ by Sugisaki and co-workers. Based on a slightly different idea, Grimsley *et al.*³¹ introduced a systematically expandable ansatz, the adaptive derivative-assembled pseudo-Trotter variational quantum eigensolver, abbreviated as ADAPT-VQE. The underlying idea behind such an ansatz is to extract most of the correlation energy with the lowest possible number of variational parameters (or fermionic excitation operators). A complementary approach for enhancing the efficiency (from the quantum complexity reduction perspective) of the VQE algorithm involves the implementation of a downfolded Hamiltonian^{32,33} or a rotated Hamiltonian^{34,35}. Few more notable works in this direction includes Unitary Cluster Jastrow (uCJ) ansatz³⁶, low rank representations³⁷, which are known to have a quadratic scaling of the parameters against the system size. Apart from the aforementioned developments in the context of traditional VQE, Stair *et al.*³⁸ introduced a variant of VQE, namely Projective Eigensolver algorithm (abbreviated as PQE). Based on the projective techniques used for solving traditional coupled cluster equations, PQE is known to carry out optimization through the residue calculations (on a quantum hardware), unlike the energy gradient calculations employed in traditional VQE.

While the success of VQE depends on the choice of parameters in the UCC ansatz, in recent times, there is an increasing interest in the many-body electronic structure community to explore the possibility of writing an N -electron correlated wavefunction with lower rank parametrization. One of the present authors had worked in this direction, and introduced a double exponential waveoperator based coupled cluster theory, which implicitly incorporates the effects of connected rank-three and rank-four excitations with only rank-one and -two parametrization, in a computationally inexpensive manner.^{39,40} In the said theory, termed as iterative n -body excitation inclusive CCSD (iCCSDn), the authors had introduced a set of rank-two scattering operators on top of the conventional single and double excitation operators. iCCSDn relies heavily on the non-commutativity of these two sets of operators, and the connected high rank excitations are simulated through the tensor contractions

between them.

With the advent of VQE algorithm for the calculations of atomic and molecular ground state energetics with a variety of unitary CC ansätze, it is compelling to verify the efficacy and accuracy of the iCCSDn methodology on a quantum architecture. As the first step towards achieving this, we develop a unitarized version of iCCSDn (UiCCSDn) theory and a number of variants thereof, and implement those on a quantum simulator for the molecular ground state energy evaluation. The various UiCCSDn variants seem to be extremely precise over the entire range of potential energy surface without a significant increase in the gate count as compared to the conventional UCCSD. This point will be elaborated towards the end of the theory section and also in the results and discussion section in the later part of the manuscript.

The paper is organized as follows: we discuss in section II the general VQE algorithm, with emphasis on the chemically motivated unitary (generalized) coupled cluster ansatz. This would be followed by a brief discussion on the conventional double exponential ansatz, iCCSDn, in section II B. In section II C, we introduce the unitarized version of the aforementioned ansatz and its various approximations along with their efficiency of implementation in the context of VQE. We will compare and contrast various aspects of (U)iCCSDn in its classical and quantum implementation. Finally, we present our results in section III, where we would study the potential energy surface of a few strongly correlated molecular systems and demonstrate that our methods can handle electronic states with varied complexity with uniform accuracy. Finally, we conclude in section IV along with a road-map to future directions.

II. THEORY

A. The variational quantum eigensolver algorithm with unitary (generalized) coupled cluster ansatz

The hybrid classical-quantum VQE algorithm uses a combination of both classical and quantum computation to find an upper bound to the ground state energy associated with a given Hamiltonian, a problem central to the field of quantum chemistry. It is based on the variational principle, and hence the ground state energy functional can be written as,

$$E(\theta) = \frac{\langle \Psi(\theta) | H | \Psi(\theta) \rangle}{\langle \Psi(\theta) | \Psi(\theta) \rangle} = \langle \Psi_{HF} | U(\theta)^\dagger H U(\theta) | \Psi_{HF} \rangle, \quad (1)$$

where $|\Psi(\theta)\rangle$ is a parameterized trial wavefunction, $|\Psi_{HF}\rangle$ is a suitable many-body reference state, which is usually the Hartree-Fock (HF) state, and H is the electronic Hamiltonian. The algorithm is divided into two subparts: the first subpart uses a quantum computer

for preparation of a parameterized wavefunction or the ansatz and measurement of the expectation value of the Hamiltonian. And the second subpart comprises of a classical optimization algorithm that minimizes the measured energy and updates the variational parameters for ansatz preparation. Thus, we can write,

$$E_0 = \min_{\theta} \langle \Psi_{HF} | U(\theta)^\dagger H U(\theta) | \Psi_{HF} \rangle, \quad (2)$$

where $U(\theta)$ is a unitary parametrized operator. The many-body molecular Hamiltonian, H , can be represented in second quantized form as shown in Eq. (3),

$$H = \sum_{p,q} h_{pq} a_p^\dagger a_q + \frac{1}{2} \sum_{p,q,r,s} h_{pqrs} a_p^\dagger a_q^\dagger a_r a_s. \quad (3)$$

One of the crucial components of VQE is the choice of the parametrized ansatz. Till date, various types of ansätze have been explored in the VQE literature. A few important things to keep in mind while selecting an ansatz are: it should be able to span the N -electron Hilbert space, and the circuit depth corresponding to the ansatz should not be beyond the reach of near term NISQ devices. One widely used ansatz is the chemically motivated UCC ansatz. It uses an unitary exponential parametrized wave operator, e^X to span the N -electron Hilbert space. There have been a number of developments along this line to judiciously choose X . In the traditional UCC method, the operator is chosen to be the sum of an excitation operator, X (defined with respect to a Fermi vacuum, usually chosen as the HF determinant) and its de-excitation counterpart, X^\dagger . The operator X (and X^\dagger) is usually truncated with rank-one and rank-two operators, giving rise to the well known UCCSD ansatz: On the other hand, the operator X may be chosen to be agnostic to the hole and particle orbitals, and one may define X to be an anti-hermitian sum of generalized rank-one and rank-two operators. This is known as the UCCGSD ansatz in the literature.

In the most general form,

$$|\Psi(\theta)\rangle_{UCC(G)SD} = e^{X(\theta) - X^\dagger(\theta)} |\Psi_{HF}\rangle; \quad (4)$$

where X is the cluster operator,

$$X = X_1 + X_2, \quad (5)$$

where

$$X_1(\theta) = \sum_{p,q} \theta_p^q a_q^\dagger a_p; \quad (6)$$

$$X_2(\theta) = \sum_{p,r;q,s} \theta_{pq}^{rs} a_s^\dagger a_q^\dagger a_r a_p. \quad (7)$$

Here, the subscripts p, q, r, s refer to general spinorbital indices for UCCGSD. If one restricts the orbitals p, r to occupied orbitals i, j and q, s to the unoccupied orbitals a, b , the UCCGSD ansatz reduces to the UCCSD one, with $X_1(\theta) \equiv T_1$, $X_2(\theta) \equiv T_2$, and $T = T_1 + T_2$. An efficient variant of the UCCGSD ansatz was proposed

by Lee *et. al.* where the authors had included only generalized pair double excitations where two electrons are “excited” from a given spatial orbital to another spatial orbital. That implies that any combination p, r from Eq. (7) have the same spatial orbital and so do their corresponding q, s . The resulting Up-CCGSD ansatz has linear circuit depth with respect to the number of spinorbitals, and is thus considered to be the current state of the art. Note that the amplitudes, θ_p^q and θ_{pr}^{qs} are the VQE parameters, which are iteratively updated through an appropriate optimizer.

In the following sections, we first present the parent iCCSDn theory from a many-body theoretic perspective and discuss its various advantages and disadvantages in its implementation on a classical computer. This would set the stage for the next section, where we would develop the unitary version of the theory and show that the unitarized version is perfectly suited to be implemented on a quantum computer.

B. The double exponential ansatz based conventional iCCSDn

In the conventional iCCSDn theory, one aims to simulate the high rank correlation effects (dominantly triples and quadruples) through a sequential similarity transformation with the exponentiated rank one and rank two operators. Towards this, one introduces a set of rank-two *scattering* operators, S , whose structure contains a true excitation in one of the vertices and a hole-hole/particle-particle scattering in another vertex. The scattering vertex contains a single (quasi-) hole or (quasi-) particle type one-electron state destruction operator. Depending on whether a hole type or a particle type of orbital that appears as the destruction operator in the scattering vertex of S , one may classify it as S_h and S_p .

$$\begin{aligned} S_h &= \frac{1}{2} \sum_{amij} s_{ij}^{am} \{a^\dagger m^\dagger j i\}; \\ S_p &= \frac{1}{2} \sum_{abie} s_{ie}^{ab} \{a^\dagger b^\dagger e i\} \quad \text{and} \\ S &= S_h + S_p. \end{aligned} \quad (8)$$

Here, a, b, c, \dots etc. denote the particle orbitals and i, j, k, \dots etc. are the hole orbitals with respect to HF determinant taken as the Fermi vacuum. In the second quantized representation of the S operators, the hole state m in S_h and the particle state e in S_p are the ones that appear as the destruction operators. Note that in the conventional CC theory with HF determinant taken as the Fermi vacuum, all the quasi-particle orbitals (e.g. a, b, c, \dots) and quasi-hole orbitals (e.g. i, j, k, \dots) appear as the creation operators. In order to distinguish the hole/particle states that appear as the destruction operator in S , we have used different symbols for them.

The S operators, due to the presence of the destruction operators, annihilate the HF reference determinant:

$S|\Psi_{HF}\rangle = 0$. This is to be referred as the *killer condition*. Furthermore, the S operators do not commute among themselves, neither do they commute with the cluster operators T . However, they have non-trivial action on an excited determinant where a given hole or particle state is created by the preceding action of an T operator. In fact, the non-commutativity between the S and the T operators are the key to simulate the connected high-rank excitations. In order to construct a terminating series of the effective Hamiltonian, in the conventional many-body formalism of iCCSDn, the S operators are not allowed to contract among themselves.

Due to the killer condition and the non-commutativity of the S and T operators, one may write down a double exponential parametrized ansatz:

$$\Omega = \{e^S\}e^{T_1+T_2}, \quad (9)$$

where the action of the two sets of exponential operators are fixed. This is to be distinguished with an ansatz like $e^{\{S\}+T}$, where the terms appearing in the exponent can appear in any order. Note that the $\{\dots\}$ denotes the normal ordering to avoid the $S-S$ contraction to ensure a naturally terminating effective Hamiltonian structure. In order to have a non-trivial coupling among S and T operators, the destruction operator in S should *necessarily* get contracted with one of the creation operators present in T .

The solutions for the optimized s and t amplitudes (corresponding to S and T operators, respectively) are done in a sequentially coupled manner. One defines the first similarity transformed effective Hamiltonian, W such that

$$\{e^S\}W = H\{e^S\} \quad (10)$$

is satisfied. Since the inverse operation of a normal ordered ansatz is not explicitly defined, one may determine W with a recursive substitution technique. The resulting structure of W takes the form:

$$W = \overbrace{\{H \exp(S)\}} - \overbrace{\{(\exp(S) - 1)H \exp(S)\}} + \overbrace{\{(\exp(S) - 1)(\exp(S) - 1)H \exp(S)\}} - \dots \quad (11)$$

This is an effective operator containing many-body terms, where usually only the rank-one and rank-two terms are retained and the series is restricted till the second term in the right hand side. With a judiciously truncated W , one may employ the second set of similarity transformation to construct double similarity transformed effective Hamiltonian $H^{eff} = e^{-T}We^T$. Note that in the double similarity transformed effective Hamiltonian, H^{eff} , both the T and S operators get coupled. Their amplitudes are determined by employing a many-body expansion and demanding that the corresponding amplitudes of H^{eff} vanish.

$$(h^{eff})_i^a = (h^{eff})_{ij}^{ab} = (h^{eff})_{ij}^{am} = (h^{eff})_{ie}^{ab} = 0. \quad (12)$$

Note that in the construction of H^{eff} , the s and the t amplitudes are iteratively optimized in a coupled manner, and as such the high rank correlation effects are simulated through the contraction between them: $T_{ijk}^{abc} \leftarrow S_{ij}^{am}T_{mk}^{bc} + S_{ie}^{ab}T_{jk}^{ec}$.

C. Unitary version of double exponential CC ansatz

1. Motivation towards the development of the unitarized ansatz

While the iCCSDn methodology is shown to be quite accurate, particularly for weakly to moderately strong correlated systems, there are a few drawbacks that it suffers from in its implementation on a classical computer.

1. The expansion in Eq. (11) (with a normal ordered ansatz as shown) is exact only up to leading order, but is naturally terminating. However, in the practical implementation, the series is usually further truncated retaining only a subset of the leading terms. That leaves out a large number of terms that otherwise could effectively contribute to the amplitude equations, Eq. (12). Furthermore, the rank of the terms appearing in the effective Hamiltonian, W is truncated to one and two-body that essentially leaves out the effects of high rank (beyond triples) excitations. Thus the ansatz with a normal ordered exponential structure has less *span* of the N -electron Hilbert space, compared to the one without the normal ordering. We must emphasise that any such theory based on many-body transformation would suffer from the unavoidable drawback.
2. While it is absolutely necessary that one adopts normal ordering and eliminates the $S-S$ contractions in order to generate a terminating series of the effective Hamiltonian, this leaves out the clustering effects, which would otherwise be present in a conventional (full) exponential structure with S .
3. The conventional iCCSDn, in practice, relies on the choice of a set of chemically active orbitals. The contractible (destruction) operators (m and e) are restricted to only those active orbitals. The cost associated with the determination of the s -amplitudes is usually dictated by the construction of the $(h^{eff})_{ie}^{ab}$ residue, which formally scales as $n_o n_v^4 n_v^{act}$. Here, n_o is the number of electrons, $n_v = (N - n_o)$ is the number of virtual spinorbitals and N is the total number of spinorbitals. $n_v^{act} = (N - n_o)^{act}$ designate the number of chemically active virtual spinorbitals (the dimension of e). This, in practice, is less than the $n_o^2 n_v^4$ which is the typical scaling of CCSD, and thus the most expensive step is still dictated by the conventional

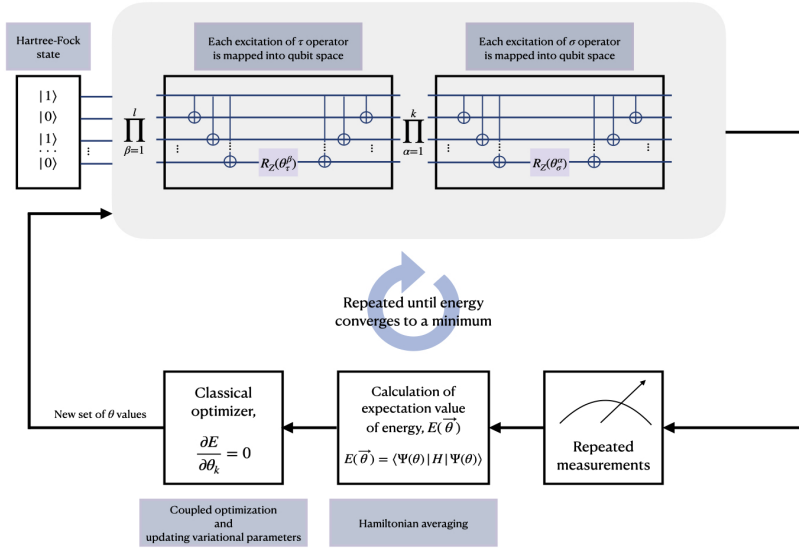


FIG. 1. Schematic illustration of the UiCCSDn scheme for an n -qubit example system. Note that each of the two circuits shown in the figure is a representative illustration of an excitation (the first block) and scattering (the second block), and does not reflect an actual full circuit, which is much deeper.

CCSD terms. One may, however, choose to expand the choice of the active space to include more occupied and/or virtual orbitals to include more complete description of the connected triple excitations at the cost of an increased computational scaling. Note that in iCCSDn, the T and the S operators are simulated through a set of *local denominators*, which can be perturbatively estimated by solving $[H_0, S^{(1)}] + V = 0$. Solution to this results in the following perturbative structure of the s -amplitudes:

$$\begin{aligned} (-\epsilon_i + \epsilon_a + \epsilon_b - \epsilon_e)(s_p)_{ie}^{ab} + v_{ie}^{ab} &= 0 \\ \Rightarrow (s_p)_{ie}^{ab} &= v_{ie}^{ab}/(\epsilon_i + \epsilon_e - \epsilon_a - \epsilon_b) \end{aligned} \quad (13)$$

and

$$(s_h)_{ij}^{am} = v_{ij}^{am}/(\epsilon_i + \epsilon_j - \epsilon_a - \epsilon_m), \quad (14)$$

where ϵ_p is the orbital energy of the p^{th} spinorbital. Thus the local energy denominator involves energies of only those orbitals that appear in a given S operator, and is equal to the energy difference between the doubly excited determinant and the triply excited determinant. While inclusion of a large number of ‘active’ orbitals generally improves the quality of the results, it also makes the theory more prone to intruders, particularly in the regions of molecular strong correlation. Thus, there is a delicate balance between the accuracy and computational scaling that one needs to maintain in order to solve the energetics of molecular systems in a uniform manner.

In order to overcome the potential drawbacks in its implementation in a classical computer as described above, it is warranted that the full exponential structure of $\exp(S)$ is utilized such that the S operators are allowed to contract among themselves. However, in such a case, the many-body first similarity transformed effective Hamiltonian W would generate exponentially large number of algebraic terms with all possible many-body ranks, which are intractable to handle on a classical computer. Also the amplitudes during the optimization process are likely to be highly plagued by the intruders, as described in point 3 above. Thus, rather than taking the many-body route, one may evolve starting from the HF reference determinant in a quantum device by means of a sequential evolution through a fixed structure double unitary ansatz and variationally optimize the energy to get the updated set of parameters.

2. Development of the unitarized iCCSDn ansatz and implementation

Towards the development of a unitary variant of iCCSDn (to be referred to as UiCCSDn henceforth) for its implementation in the VQE framework, the normal ordering of e^S is removed by the conventional exponential structure and the S operators are replaced by an anti-Hermitian sum of S and S^\dagger . Similarly, the T operators are replaced by the anti-Hermitian sum of the excitation

operator (T itself) and the de-excitation operators (T^\dagger):

$$\begin{aligned} S_h &\rightarrow S_h - S_h^\dagger = \sigma_h : (\sigma_h)_{ij}^{am} = (S_h)_{ij}^{am} - (S_h)_{am}^{ij} \\ S_p &\rightarrow S_p - S_p^\dagger = \sigma_p : (\sigma_p)_{ie}^{ab} = (S_p)_{ie}^{ab} - (S_p)_{ab}^{ie} \\ T_2 &\rightarrow T_2 - T_2^\dagger = \tau_2 : \tau_{ij}^{ab} = T_{ij}^{ab} - T_{ab}^{ij} \\ T_1 &\rightarrow T_1 - T_1^\dagger = \tau_1 : \tau_i^a = T_i^a - T_a^i. \end{aligned} \quad (15)$$

Thus, in Eq. (9), both the exponential terms can be replaced by their unitary counterparts:

$$U = U_1 U_2 = \exp(\sigma) \exp(\tau), \quad (16)$$

where $\sigma = \sigma_h + \sigma_p$ and $\tau = \tau_1 + \tau_2$. Note that due to the exponential structure, the effective Hamiltonian can in principle be expanded in the Baker-Campbell-Hausdorff expansion to obtain normalized Hamiltonian expectation value with variational optimization. However, due to the contraction among various components of the ansatz, the BCH expansion is non-terminating, making it intractable on a classical computer.

The unitary version of iCCSDn may be employed to study the coherent time evolution in a quantum computer. Towards this, the ansatz is broken down into several time ordered sequences of few-particle operators using Trotter expansion. One may note that the S and the T operators do not commute in general. Since we have started with a double unitary structure and the σ and τ operators do not commute, $e^\sigma e^\tau \neq e^{\sigma+\tau}$. However, from each set of operators, one may group terms which are mutually commuting such that

$$e^{\sigma_A + \sigma_B} e^{\tau_A + \tau_B} = \left(\lim_{\rho \rightarrow \infty} (e^{\sigma_A/\rho} e^{\sigma_B/\rho})^\rho \right) \times \left(\lim_{\lambda \rightarrow \infty} (e^{\tau_A/\lambda} e^{\tau_B/\lambda})^\lambda \right). \quad (17)$$

Although a truncated Trotter expansion of the set of non-commuting operators is an approximation in the UiCCSDn wavefunction, the choice of the operators provide us with enough variational flexibility to simulate strongly correlated systems. Even with $\rho = \lambda = 1$ and a suitably approximated σ operator, it can reproduce results which are well within the limit of chemical accuracy, irrespective of the degree of correlation of the system. The Trotterized ansatz thus takes a form:

$$|\Psi_{UiCCSDn}\rangle = \left(\prod_{q \in \{q_h, q_p\}} e^{\sigma_q} \prod_{r \in \{q_1, q_2\}} e^{\tau_r} \right) |\Psi_{HF}\rangle. \quad (18)$$

Here, q_h and q_p are the unique quartet of all (i, j, a, m) and (i, e, a, b) respectively, and r takes the unique combinations of all singles and doubles. This is realized through a concatenated quantum circuit where e^τ (with selection of τ operators in lexical ordering) acts on the HF state first, followed by e^{σ_h} and e^{σ_p} (with selection of the σ_h and σ_p operators in lexical ordering among themselves). One may further increase the variational flexibility of the ansatz by independently taking a product of k

and l number of e^σ and e^τ unitary circuits, respectively. The ansatz thus takes a generalized form:

$$|\Psi_{UiCCSDn}\rangle = \left(\prod_{\alpha=1}^k \prod_{q \in \{q_h, q_p\}} e^{\sigma_q^{(\alpha)}} \right) \times \left(\prod_{\beta=1}^l \prod_{r \in \{q_1, q_2\}} e^{\tau_r^{(\beta)}} \right) |\Psi_{HF}\rangle. \quad (19)$$

Here $\sigma_q^{(\alpha)}$ and $\tau_r^{(\beta)}$ are treated as independent parameters. We will show that for a few specific variants, the circuit for e^σ is quite shallow (*vide infra*), allowing us to increase the value of k (keeping $l = 1$) without significant increase in the circuit depth. A schematic representation of the quantum circuit is shown in Fig. 1 below.

One may note that choosing the ansatz through a double unitary has an added advantage over a single unitary where one may write the unitary evolution operator as $e^{\sigma+\tau}$. In the first order Trotter decomposition, although both ways of writing the ansatz may superficially look similar, in our double unitary case, the order of the action of e^σ and e^τ are fixed, contrary to a single unitary. For the single unitary ansatz like $e^{\sigma+\tau}$, one needs to optimize the order of appearance of various terms in the circuit. Typically, those operators should be allowed to act on the HF state first which do not annihilate the reference. In our case, e^σ , by construction, is allowed to act on the entangled state, $e^\tau |\Psi_{HF}\rangle$. It was found that the energy depends on the ordering of the operators even among the two separate circuits; however, in the current study both τ and σ operators are taken in their lexical ordering. One may also note that our ansatz allows us to repeat a part of the whole circuit to improve accuracy in a systematic manner.

3. Various approximate UiCCSDn schemes and the associated resource estimation

In this section, we will introduce a number of variants of UiCCSDn ansatz, in which we will judiciously approximate the S operators such that the resulting ansätze strikes the right balance between expressibility, accuracy, number of parameters and circuit depth. We will also justify our choice from the perspective of many-body perturbation theory. Noting the fact that our scheme is not agnostic to the choice of holes and particles, we comment that the introduction of an operator with structures like that of S is the minimal requirement to introduce connected high-rank correlation effects beyond singles and doubles, and thus the resulting ansatz is expected to bring in better span of the Hilbert space. Furthermore, one may significantly cut down the number of free parameters (and gate count) by restricting the contractible orbitals (which appears as the quasi-hole/particle destruction operator) to some chemically *active* ones. We introduce the variants below which differ from each other in

Variants	Choice of σ	Description
UiCCSDn	$\{(\sigma_h)_{ij}^{am}, (\sigma_p)_{ie}^{ab}\}$	1. Untruncated.
UiCCSDn-A	$\{(\sigma_h)_{ij}^{au}, (\sigma_p)_{iv}^{ab}\}$	1. Active orbitals.
UiCCSDn-A-op	$\{(\sigma_h)_{i_\alpha j_\beta}^{a_\alpha u_\beta}, (\sigma_h)_{i_\beta j_\alpha}^{a_\beta u_\alpha};$ $(\sigma_p)_{i_\alpha v_\beta}^{a_\alpha b_\beta}, (\sigma_p)_{i_\beta v_\alpha}^{a_\beta b_\alpha}\}$	1. Active orbitals. 2. Opposite spin in scattering and excitation vertex of σ .
UiCCSDn-A-diag	$\{(\sigma_h)_{iu}^{au}, (\sigma_p)_{iv}^{ab}\}$	1. Active orbitals. 2. Diagonal terms in scattering vertex of σ .
UiCCSDn-A-pp	$\{(\sigma_h)_{i_\alpha i_\beta}^{a_\alpha u_\beta}, (\sigma_h)_{i_\beta i_\alpha}^{a_\beta u_\alpha};$ $(\sigma_p)_{i_\alpha v_\beta}^{a_\alpha b_\beta}, (\sigma_p)_{i_\beta v_\alpha}^{a_\beta b_\alpha}\}$	1. Active orbitals. 2. Same spatial orbitals for quasi-hole (in σ_h) and quasi-particle (in σ_p).

TABLE I. Summary of various approximate UiCCSDn schemes depending on the choice of the σ operators. The cluster operator τ is taken to be all $1h - 1p$ and $2h - 2p$ excitations without any further truncation.

Ansatz	T_1	T_2	T_3	S_h	S_p	Gate depth
UCCSD	$\mathcal{O}(n_o n_v)$	$\mathcal{O}(n_o^2 n_v^2)$	-	-	-	$\mathcal{O}(n_o n_v^2)$
UCCSDT	$\mathcal{O}(n_o n_v)$	$\mathcal{O}(n_o^2 n_v^2)$	$\mathcal{O}(n_o^3 n_v^3)$	-	-	$\mathcal{O}(n_o^2 n_v^3)$
UiCCSDn	$\mathcal{O}(n_o n_v)$	$\mathcal{O}(n_o^2 n_v^2)$	-	$\mathcal{O}(n_o^3 n_v)$	$\mathcal{O}(n_o n_v^3)$	$\mathcal{O}(n_v^3)$
UiCCSDn-A	$\mathcal{O}(n_o n_v)$	$\mathcal{O}(n_o^2 n_v^2)$	-	$\mathcal{O}(n_o^2 n_v n_o^{act})$	$\mathcal{O}(n_o n_v^2 n_v^{act})$	$\mathcal{O}(n_o n_v^2)$
UiCCSDn-A-op	$\mathcal{O}(n_o n_v)$	$\mathcal{O}(n_o^2 n_v^2)$	-	$\mathcal{O}(\frac{1}{16} n_o^2 n_v n_o^{act})$	$\mathcal{O}(\frac{1}{16} n_o n_v^2 n_v^{act})$	$\mathcal{O}(n_o n_v^2)$
UiCCSDn-A-diag	$\mathcal{O}(n_o n_v)$	$\mathcal{O}(n_o^2 n_v^2)$	-	$\mathcal{O}(n_o n_v n_o^{act})$	$\mathcal{O}(n_o n_v n_v^{act})$	$\mathcal{O}(n_o n_v^2)$
UiCCSDn-A-pp	$\mathcal{O}(n_o n_v)$	$\mathcal{O}(n_o^2 n_v^2)$	-	$\mathcal{O}(\frac{1}{8} n_o n_v n_o^{act})$	$\mathcal{O}(\frac{1}{8} n_o n_v n_v^{act})$	$\mathcal{O}(n_o n_v^2)$

TABLE II. The number of parameters (and gates) required for each class of operators for the implementation of UCCSD, UCCSDT and various UiCCSDn variants. The leading gate count for each of the ansatz are highlighted and put in the bold text. Also the corresponding leading gate depth is reported. Note that UiCCSDn variants have much fewer number of gates required than UCCSDT.

the choice of the scattering component in σ . Please note that in all the variants, the hole-particle structure of τ is retained in full.

- UiCCSDn:** In the parent UiCCSDn theory, both the σ and τ operators are retained in full and there is no further approximation involved. That implies that the contractible set of orbitals m and e in σ_h and σ_p respectively are taken to be all the occupied and unoccupied orbitals. Implementation of the parent (untruncated) UiCCSDn requires $\mathcal{O}(n_o^3 n_v)$ σ_h and $\mathcal{O}(n_o n_v^3)$ σ_p parameters on top of the conventional $\mathcal{O}(n_o^2 n_v^2)$ elements of τ . Note that the leading order of parameter count and gate count are dictated by the number of σ_p elements, while the circuit depth scales as $\mathcal{O}(n_v^3)$.
- UiCCSDn-A:** In this variant, the contractible (hole and particle) orbital indices are restricted to the chemically active orbitals. Since in our ansatz, the high-rank correlation is simulated through the contraction of the S and the T operators, we span the full N -electron Hilbert space through only those S operators which involve contractible orbitals near the Fermi level. Note that in this

variant, there is no loss in the expressibility of the ansatz as it spans the full N -electron Hilbert space; however, they are generated through a selected contraction of the most dominant σ with the τ amplitudes.

$$\sigma_{UiCCSDn-A} \in \{(\sigma_h)_{ij}^{au}, (\sigma_p)_{iv}^{ab}\} \quad (20)$$

where u and v are the ‘‘active’’ hole and particle orbital lines, respectively. Noting the fact that $n_o^{act}, n_v^{act} \ll n_o, n_v$, the parameter count is $\mathcal{O}(n_o^2 n_v^2)$ due to τ . The circuit depth scales $\mathcal{O}(n_o n_v^2)$.

- UiCCSDn-A-op:** On top of the selection of the active orbitals as the contractible indices, we only incorporate those σ operators in which the spins in the excitation vertex and the scattering vertex of σ are different. This implies that some of the high-spin correlation channels are switched off.

$$\sigma_{UiCCSDn-A-op} \in \{(\sigma_h)_{i_\alpha j_\beta}^{a_\alpha u_\beta}, (\sigma_h)_{i_\beta j_\alpha}^{a_\beta u_\alpha};$$

$$(\sigma_p)_{i_\alpha v_\beta}^{a_\alpha b_\beta}, (\sigma_p)_{i_\beta v_\alpha}^{a_\beta b_\alpha}\} \quad (21)$$

u and v denote active spatial occupied and virtual orbitals, and α and β denote the spin-up and spin-down electrons, respectively. While the number of σ_h and σ_p parameters in the UiCCSDn-A-op variant scale similar to UiCCSDn-A, there is a small pre-factor of 1/16 in the former case. Thus for practical applications of UiCCSDn-A-op, there is a tremendous reduction in the number of the free parameters over the UiCCSDn-A variant. While this requires $\mathcal{O}(\frac{1}{16}n_o^2n_vn_o^{act})$ number of σ_h and $\mathcal{O}(\frac{1}{16}n_on_vn_v^{act})$ number of σ_p parameters, the parameter count is, however, dictated by $\mathcal{O}(n_o^2n_v^2)$ number of τ amplitudes with a circuit depth of $\mathcal{O}(n_on_v^2)$.

4. **UiCCSDn-A-diag:** Note that the orbitals involved in the scattering vertex of S appear with opposite signs in their perturbative energy denominator (see Eqs. (13) and (14)). One may thus decipher that the most dominant terms in S (or σ) are those which have diagonal scattering. In the UiCCSDn-A-diag variant, we thus restrict the orbitals involved in the scattering vertex of σ to be the same. Inclusion of diagonal terms in the scattering vertex reduces the computation cost of Jordan-Wigner overhead significantly.

$$\sigma_{\text{UiCCSDn-A-diag}} \in \{(\sigma_h)_{iu}^{au}; (\sigma_p)_{iv}^{av}\} \quad (22)$$

The number of σ_h and σ_p parameters are further reduced to $\mathcal{O}(n_on_vn_o^{act})$ number of σ_h and $\mathcal{O}(n_on_vn_v^{act})$ number of σ_p elements. The leading parameter count thus still scales as $\mathcal{O}(n_o^2n_v^2)$ with a circuit depth of $\mathcal{O}(n_on_v^2)$.

5. **UiCCSDn-A-pp:** In the UiCCSDn-A-pp variant (where “pp” stands for partial pairing), in addition to the active orbital selection in the destruction component of S , we include (i) only those quasi-hole creation operators which originate from the same spatial orbitals (for σ_h) and (ii) only those quasi-particle creation operators which have the same spatial orbitals (for σ_h).

$$\sigma_{\text{UiCCSDn-A-pp}} \in \{(\sigma_h)_{i_\alpha i_\beta}^{a_\alpha a_\beta}, (\sigma_h)_{i_\beta i_\alpha}^{a_\beta a_\alpha}; (\sigma_p)_{i_\alpha v_\beta}^{a_\alpha a_\beta}, (\sigma_p)_{i_\beta v_\alpha}^{a_\beta a_\alpha}\} \quad (23)$$

Note that there is only partial pairing either among the quasi-hole or quasi-particle orbitals and the structure of the σ operators does not allow to have complete pairing. This variant further lowers the number of σ_h and σ_p elements over UiCCSDn-A-diag and the gate count and the circuit depth scales similar to UiCCSDn-A-diag.

One may note that in all the variants, except the parent (untruncated) UiCCSDn, there is no increase in the order of the gate count and circuit depth over the conventional UCCSD. However, we will demonstrate that all

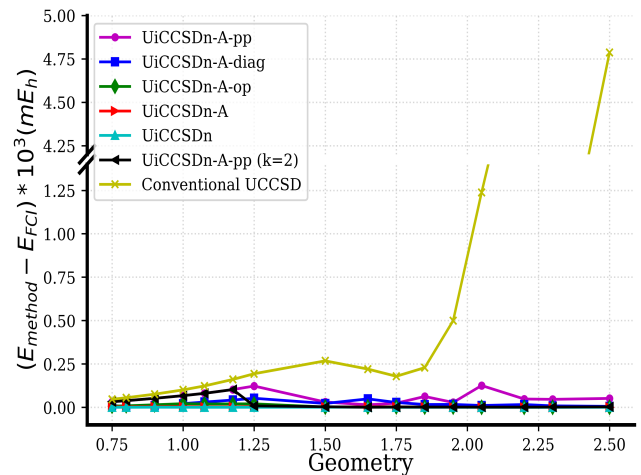


FIG. 2. Difference between VQE energies corresponding to various ansätze and FCI energies for H_2O at symmetric stretching in STO-3G basis.

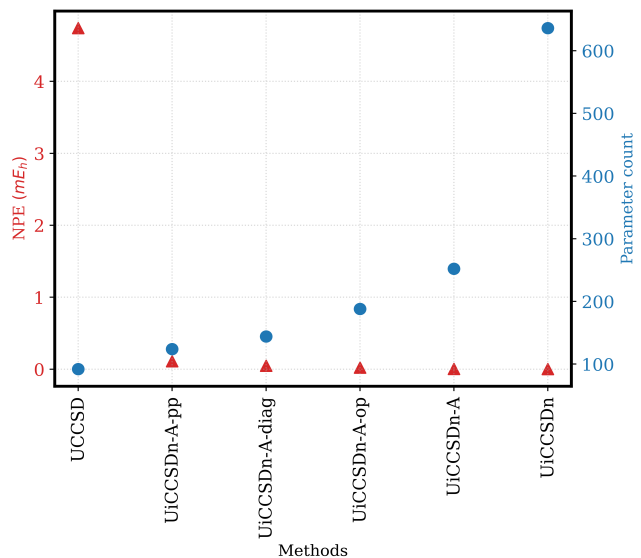


FIG. 3. Non-parallelity error (red triangles) and parameters count (blue dots) corresponding to various ansätze for the symmetric stretching of H_2O in STO-3G basis.

our variants predict energy well within the chemical accuracy. A succinct summary of the choice of the various operators and the associated parameter count in different approximate schemes are given in Table. I and II respectively.

III. RESULTS AND DISCUSSIONS

A. Methodology

We have chosen to study the potential energy surface for symmetric stretching of H_2O and LiH to assess the

Method	Energy (E_h)			
	d=1Å	d=2Å	d=3Å	d=4Å
FCI	-7.78446028	-7.86108777	-7.79884316	-7.78427817
UCCSD	-7.78445508 (0.0052)	-7.86106905 (0.0187)	-7.79875361 (0.0895)	-7.78414449 (0.1336)
UiCCSDn-A-pp	-7.78445982 (0.0004)	-7.86108722 (0.0005)	-7.79884258 (0.0005)	-7.78427777 (0.0004)
UiCCSDn-A-diag	-7.78446017 (0.0001)	-7.86108736 (0.0004)	-7.79884162 (0.0015)	-7.78427446 (0.0037)
UiCCSDn-A-op	-7.78446000 (0.0002)	-7.86108766 (0.0001)	-7.79884256 (0.0006)	-7.78427780 (0.0003)
UiCCSDn-A	-7.78446025 (0.0000)	-7.86108772 (0.0000)	-7.79884302 (0.0001)	-7.78427781 (0.0003)

TABLE III. The energy values (in E_h) for some selected geometries of LiH molecule using UCCSD and different UiCCSDn variants. The corresponding FCI energy values are also reported to demonstrate the accuracy of our schemes. The quantities in parenthesis denote the energy difference (in mE_h) from the FCI values. Note that all the energy values reported here used $k = l = 1$.

performance of the newly developed UiCCSDn ansatz and the subsequent variants in the context of VQE. For all our computations, we have chosen the contracted STO-3G basis⁴¹. The one- and two- electron integrals were taken from PySCF⁴², and the UiCCSDn ansatz has been implemented in Qiskit 0.26⁴³. Also, the UCCSD calculations were done using the same version of Qiskit whereas the UCCSDT calculations were carried out in Qiskit nature. The Jordan-Wigner scheme⁴⁴ was chosen for encoding the creation and annihilation operators into the qubit operators. Also, we had employed the direct spin-orbital to qubit mapping: that is each spin-orbital is represented as one qubit, independent of the occupancy of the spin-orbitals. For the classical subpart of the VQE, we chose L_BFGS_B optimizer⁴⁵ throughout. For all the calculations, the initial values of all the parameters, θ_{init} , were set to zero. Further, in the present study, we have worked with the statevector backend simulator. The Trotter number for all our calculations was set to be one.

B. Symmetric stretching of H_2O

1. The potential energy surface and the non-parallelity error

We determined the VQE energies employing our ansätze for all the geometries along the potential energy surface. We have varied the O-H bond length from around 0.75 times the equilibrium distance to 2.5 times the equilibrium distance in order to generate the potential energy surface. For the purpose of comparison, we have also computed the VQE energies using the conventional UCCSD ansatz. As shown in Fig. 2, we have plotted the differences between the VQE energies computed using the aforementioned ansätze and the FCI

energies. It is quite evident from the plot that VQE with the conventional UCCSD ansatz performs quite well and agrees to 0.18 milliHartree (mE_h) with respect to FCI, for geometries below 1.75 times the equilibrium length, but starts deviating beyond that point. This trend shows that for the domains where strong correlation effects come into play, UCCSD fails to estimate the ground state energies. Whereas the energies obtained using the UiCCSDn-A-pp ansatz (which is the least parametrized ansatz amongst our other ansätze) are precise up to tens of microHartree ($\sim 10\mu E_h$) throughout the potential energy surface. In order to explicate our observations, we have further calculated the corresponding non-parallelity error, abbreviated as NPE. NPE is defined as the difference between the maximum and minimum deviations from the exact ground state energy, i.e., FCI in our case. We observe that the NPE corresponding to the conventional UCCSD and UCCSDT ansatz is 4.74 mE_h and 2.169 mE_h respectively. On the other hand, the NPE associated with the least parametrized ansatz, UiCCSDn-A-pp, is found to be 0.11 mE_h . The NPE and the parameters count associated with all the ansätze have been plotted in Fig. 3.

In order to assess the efficiency of the newly developed ansätze, it is important to elucidate on the circuit complexity, which is quantified by the number of variational parameters and the quantum gate count. We should note that the NPE corresponding to UiCCSDn-A-pp is in the order of 0.11 mE_h at the expense of an additional 32 parameters over the conventional UCCSD (with a NPE of 4.74 mE_h). Also it is worth mentioning at this point that the conventional UCCSDT leads to a NPE of 2.169 mE_h at the expense of 188 parameters (which is of the order $\sim \mathcal{O}(n_o^3 n_v^3)$), whereas the UiCCSDn-A-diag (with lesser number of parameters than UCCSDT) and the UiCCSDn-A-op (with same number of parameters as

UCCSDT) exhibit $0.048 mE_h$ and $0.0209 mE_h$ NPE respectively. Looking at the number of parameters (and hence, the gate count), we can infer that the newly developed ansätze strikes a right balance between the two aspects i.e., implementation cost and the accuracy.

C. Potential energy curve for LiH dissociation

We have evaluated the VQE energies employing different variants of UiCCSDn ansätze for a few selected geometries of LiH, as listed in Table III. According to our findings, the conventional UCCSD approach performs pretty well around the equilibrium geometry, but it starts to deteriorate for the strongly correlated regions when the $Li-H$ bond is stretched. However, the ground state energies evaluated through our ansätze uniformly show a sub micro-hartree accuracy for both weakly and strongly correlated regions irrespective of the UiCCSDn variant.

IV. CONCLUSION AND FUTURE OUTLOOK

In this paper, we have developed the unitary version of the dual exponential coupled cluster methodology (UiCCSDn) and have adapted it for use in a quantum computing framework. We have presented theoretical arguments for the non-viability of implementing the iCCSDn methodology or for that matter, its unitary version on a classical device without approximation in the rank and number of terms in the similarity transformed many-body Hamiltonian. The implementation of UiCCSDn in a quantum device can bypass these drawbacks entirely. The dual exponential structure, by construction, allows the scattering operators to act on entangled states to induce high-rank excitations. We have introduced different variants by judiciously including a selection of the scattering operators while keeping the cluster operators in full. Apart from the parent UiCCSDn, all the variants have a gate count and circuit depth in the same order as the conventional UCCSD without significantly compromising the expressibility of the ansätze. We have shown with a prototypical molecular application that all the different variants show high accuracy compared to classically computed FCI over the entire molecular surface, but with a significantly less implementation cost than allied theories.

It would be interesting to implement the UiCCSDn in the ADAPT-VQE framework to further reduce the parameter count. Evaluation of the parameters in PQE framework would be another avenue which would keep us engaged in coming years.

V. ACKNOWLEDGEMENTS

RM thanks Science and Engineering Research Board (SERB), Government of India for providing financial support. DH thanks SERB and IRCC, IIT Bombay for research fellowship. Some of the preliminary calculations were carried out on National Supercomputing Mission's (NSM) computing resource, 'PARAM Siddhi-AI', at C-DAC Pune, which is implemented by C-DAC and supported by the Ministry of Electronics and Information Technology (MeitY) and Department of Science and Technology (DST), Government of India.

DATA AVAILABILITY

The data generated in this study is available upon reasonable request to the corresponding author.

- ¹D. Deutsch and R. Jozsa, Rapid Solution of Problems by Quantum Computation, Proc. Royal Soc. London Series A **439**, 553 (1992).
- ²P. W. Shor, Polynomial-Time Algorithms for Prime Factorization and Discrete Logarithms on a Quantum Computer, SIAM J. Comp. **26**, 1484 (1997).
- ³G. Ortiz, J. E. Gubernatis, E. Knill and R. Laflamme, Quantum Algorithms for Fermionic Simulations, Phys. Rev. A **64**, 022319 (2001).
- ⁴A. W. Harrow, A. Hassidim and S. Lloyd, Quantum Algorithm for Linear Systems of Equations, Phys. Rev. Lett. **103**, 150502 (2009).
- ⁵Y. Cao, J. Romero, J. P. Olson, M. Degroote, P. D. Johnson, M. Kieferová, I. D. Kivlichan, T. Menke, B. Peropadre, N. P. D. Sawaya, S. Sim, L. Veis and A. Aspuru-Guzik, Quantum Chemistry in the Age of Quantum Computing, Chem. Rev. **119**, 10856 (2019).
- ⁶S. McArdle, S. Endo, A. Aspuru-Guzik, S. Benjamin and X. Yuan, Quantum Computational Chemistry, Rev. Mod. Phys. **92**, 15003 (2020).
- ⁷D. S. Abrams and S. Lloyd, Simulation of Many-Body Fermi Systems on a Universal Quantum Computer, Phys. Rev. Lett. **79**, 2586 (1997).
- ⁸D. S. Abrams and S. Lloyd, Quantum Algorithm Providing Exponential Speed Increase for Finding Eigenvalues and Eigenvectors, Phys. Rev. Lett. **83**, 5162 (1999).
- ⁹A. Aspuru-Guzik, A. D. Dutoi, P. J. Love and M. Head-Gordon, Simulated Quantum Computation of Molecular Energies, Science **309**, 1704 (2005).
- ¹⁰H. Wang, S. Kais, A. Aspuru-Guzik and M. R. Hoffmann, Quantum Algorithm for Obtaining the Energy Spectrum of Molecular Systems, Phys. Chem. Chem. Phys. **10**, 5388 (2008).
- ¹¹L. Veis and J. Pittner, Quantum Computing Applied to Calculations of Molecular Energies: CH₂ Benchmark, J. Chem. Phys. **133**, 194106 (2010).
- ¹²K. Sugisaki, S. Nakazawa, K. Toyota, K. Sato, D. Shiomi and T. Takui, Quantum Chemistry on Quantum Computers: A Method for Preparation of Multiconfigurational Wave Functions on Quantum Computers without Performing Post-Hartree-Fock Calculations, ACS Cent. Sci. **5**, 167 (2019).
- ¹³D. Halder, V. S. Prasanna, V. Agarawal and R. Maitra, Digital Quantum Simulation of Strong Correlation Effects with Iterative Quantum Phase Estimation Over the Variational Quantum Eigensolver Algorithm: H_4 on a circle as a case study, preprint at arXiv:2110.02864 (2021).
- ¹⁴A. Peruzzo, J. McClean, P. Shadbolt, M. H. Yung, X. Q. Zhou, P. J. Love, A. Aspuru-Guzik and J. L. O'Brien, A Varia-

- tional Eigenvalue Solver on a Photonic Quantum Processor, *Nat. Comm.* **5**, 4213 (2014).
- ¹⁵D. J. Griffiths, *Introduction to Quantum Mechanics*, 2nd Ed., Chapter 7 (2005).
 - ¹⁶P. J. J. O'Malley, R. Babbush, I. D. Kivlichan, J. Romero, J. R. McClean, R. Barends, J. Kelly, P. Roushan, A. Tranter, N. Ding, B. Campbell, Y. Chen, Z. Chen, B. Chiaro, A. Dunsworth, A. G. Fowler, E. Jeffrey, E. Lucero, A. Megrant, J. Y. Mutus, M. Neeley, C. Neill, C. Quintana, D. Sank, A. Vainsencher, J. Wenner, T. C. White, P. V. Coveney, P. J. Love, H. Neven, A. Aspuru-Guzik and J. M. Martinis, Scalable Quantum Simulation of Molecular Energies, *Phys. Rev. X* **6**, 031007 (2016).
 - ¹⁷J. I. Colless, V. V. Ramasesh, D. Dahlen, M. S. Blok, M. E. Kimchi-Schwartz, J. R. McClean, J. Carter, W. A. de Jong and I. Siddiqi, Computation of Molecular Spectra on a Quantum Processor with an Error-Resilient Algorithm, *Phys. Rev. X* **8**, 011021 (2018).
 - ¹⁸Y. Shen, X. Zhang, S. Zhang, J.-N. Zhang, M.-H. Yung and K. Kim, Quantum Implementation of the Unitary Coupled Cluster for Simulating Molecular Electronic structure, *Phys. Rev. A* **95**, 020501 (2017).
 - ¹⁹C. Hempel, C. Maier, J. Romero, J. McClean, T. Monz, H. Shen, P. Jurcevic, B. P. Lanyon, P. Love, R. Babbush, A. Aspuru-Guzik, R. Blatt and C. F. Roos, Quantum Chemistry Calculations on a Trapped-Ion Quantum Simulator, *Phys. Rev. X* **8**, 031022 (2018).
 - ²⁰C. Kokail, C. Maier, R. van Bijnen, T. Brydges, M. K. Joshi, P. Jurcevic, C. A. Muschik, P. Silvi, R. Blatt, C. F. Roos and P. Zoller, Self-Verifying Variational Quantum Simulation of Lattice Models, *Nature* **569**, 355 (2019).
 - ²¹W. Kutzelnigg, Error Analysis and Improvements of Coupled-Cluster Theory, *Theoret. Chim. Acta* **80**, 349 (1991).
 - ²²M. H. Yung, J. Casanova, A. Mezzacapo, J. McClean, L. Lamata, A. Aspuru-Guzik and E. Solano, From Transistor to Trapped-Ion Computers for Quantum Chemistry, *Sci. Rep.* **4**, 3589 (2014).
 - ²³F. A. Evangelista, G.K.-L. Chan and G. E. Scuseria, Exact Parameterization of Fermionic Wave Functions via Unitary Coupled Cluster Theory, *J. Chem. Phys.* **151**, 244112 (2019).
 - ²⁴J. Romero, R. Babbush, J. R. McClean, C. Hempel, P. J. Love and A. Aspuru-Guzik, Strategies for Quantum Computing Molecular Energies Using the Unitary Coupled Cluster Ansatz, *Quantum Sci. Technol.* **4**, 014008 (2018).
 - ²⁵A. Anand, P. Schleich, S. Alperin-Lea, P. W. K. Jensen, S. Sim, M. Diaz-Tinoco, J. S. Kottmann, M. Degroote, A. F. Izmaylov and A. Aspuru-Guzik, A Quantum Computing View on Unitary Coupled Cluster Theory, *Chem. Soc. Rev.* **51**, 1659 (2022).
 - ²⁶H. Nakatsuji, Equation for the Direct Determination of the Density Matrix, *Phys. Rev. A* **14**, 41 (1976).
 - ²⁷M. Nooijen, Can the Eigenstates of a Many-Body Hamiltonian Be Represented Exactly Using a General Two-Body Cluster Expansion?, *Phys. Rev. Lett.* **84**, 2108 (2000).
 - ²⁸T. V. Voorhis and M. Head-Gordon, Two-body Coupled Cluster Expansions, *J. Chem. Phys.* **115**, 5033 (2001).
 - ²⁹J. Lee, W. J. Huggins, M. Head-Gordon and K. B. Whaley, Generalized Unitary Coupled Cluster Wave functions for Quantum Computation, *J. Chem. Theory Comput.* **15**, 311 (2019).
 - ³⁰K. Sugisaki, T. Kato, Y. Minato, K. Okuwaki and Y. Mochizuki, Variational Quantum Eigensolver Simulations with the Multireference Unitary Coupled Cluster Ansatz: A Case Study of the C_{2v} Quasi-Reaction Pathway of Beryllium Insertion into a H_2 Molecule, *Phys. Chem. Chem. Phys.* **24**, 8439 (2022).
 - ³¹H. R. Grimsley, S. E. Economou, E. Barnes and N. J. Mayhall, An Adaptive Variational Algorithm for Exact Molecular Simulations on a Quantum Computer, *Nat. Commun.* **10**, 3007 (2019).
 - ³²N. P. Bauman and K. Kowalski, Coupled Cluster Downfolding Theory: Towards Universal Many-Body Algorithms for Dimensionality Reduction of Composite Quantum Systems in Chemistry and Materials Science, *Mater. Theory.* **6**, 17 (2022).
 - ³³M. Metcalf, N. P. Bauman, K. Kowalski and W. A. de Jong, Resource-Efficient Chemistry on Quantum Computers with the Variational Quantum Eigensolver and the Double Unitary Coupled-Cluster Approach, *J. Chem. Theory Comput.* **16**, 6165 (2020).
 - ³⁴I. O. Sokolov, P. K. Barkoutsos, P. J. Ollitrault, D. Greenberg, J. Rice, M. Pistoia and I. Tavernelli, Quantum Orbital-Optimized Unitary Coupled Cluster Methods in the Strongly Correlated Regime: Can Quantum Algorithms Outperform their Classical Equivalents?, *J. Chem. Phys.* **152**, 124107 (2020).
 - ³⁵W. Mizukami, K. Mitarai, Y. O. Nakagawa, T. Yamamoto, T. Yan and Y.-y. Ohnishi, Orbital Optimized Unitary Coupled Cluster Theory for Quantum Computer, *Phys. Rev. Research* **2**, 033421 (2020).
 - ³⁶Y. Matsuzawa and Y. Kurashige, Jastrow-type Decomposition in Quantum Chemistry for Low-Depth Quantum Circuits, *J. Chem. Theory Comput.* **16**, 944 (2020).
 - ³⁷M. Motta, E. Ye, J. R. McClean, Z. Li, A. J. Minnich, R. Babbush and G. K.-L. Chan, Low rank representations for quantum simulation of electronic structure, *NPJ Quantum Inf.* **7**, 83 (2021).
 - ³⁸N. H. Stair and F. A. Evangelista, Simulating Many-Body Systems with a Projective Quantum Eigensolver, *PRX Quantum* **2**, 030301 (2021).
 - ³⁹R. Maitra, Y. Akinaga and T. Nakajima, A coupled cluster theory with iterative inclusion of triple excitations and associated equation of motion formulation for excitation energy and ionization potential, *J. Chem. Phys.* **147**, 074103 (2017).
 - ⁴⁰S. Tribedi, A. Chakraborty and R. Maitra, Formulation of a Dressed Coupled-Cluster Method with Implicit Triple Excitations and Benchmark Application to Hydrogen-Bonded Systems, *J. Chem. Theory Comput.* **16**, 6317 (2020).
 - ⁴¹W. J. Hehre, R. F. Stewart and J. A. Pople, Self-Consistent Molecular-Orbital Methods. I. Use of Gaussian Expansions of Slater-Type Atomic Orbitals, *J. Chem. Phys.* **51**, 2657 (1969).
 - ⁴²Q. Sun *et. al.*, PySCF: The Python-Based Simulations of Chemistry Framework, *Wiley Interdisciplinary Reviews: Computational Molecular Science*, **8**, e1340 (2017).
 - ⁴³H. Abraham *et. al.*, Qiskit: An Open-source Framework for Quantum Computing, 10.5281/zenodo.2562110 (2019).
 - ⁴⁴J. T. Seeley, M. J. Richard and P. J. Love, The Bravyi-Kitaev Transformation for Quantum Computation of Electronic Structure, *J. Chem. Phys.* **137**, 224109 (2012).
 - ⁴⁵R. Byrd, P. Lu, J. Nocedal and C. Zhu, Limited Memory Algorithm for Bound Constrained Optimization, *SIAM J. Sci. Comput.* **16**, 1190 (1995).
 - ⁴⁶A. Dutta and C. D. Sherrill, Full Configuration Interaction Potential Energy Curves for Breaking Bonds to Hydrogen: An Assessment of Single-Reference Correlation Methods, *J. Chem. Phys.* **118**, 1610 (2003).